



## The use of NaX zeolite as a template to obtain a mono-atomic Pt dispersion by impregnation with Pt(II) acetylacetone/acetone solution

SLAVKO MENTUS<sup>1\*</sup>#, ZORICA MOJOVIĆ<sup>2</sup> and VELIMIR RADMILOVIĆ<sup>3</sup>

<sup>1</sup>University of Belgrade, Faculty of Physical Chemistry, Studentski trg 12, 11000 Belgrade,

<sup>2</sup>ICTM – Department for Catalysis and Chemical Engineering, Njegoševa 12, 11000

Belgrade, Serbia and <sup>3</sup>National Center for Electron Microscopy, Lawrence Berkeley

National Laboratory, University of California, Berkeley, USA

(Received 26 October 2008, revised 11 June 2009)

**Abstract:** The incorporation of platinum into the cavities of NaX zeolite was realized by impregnation and thermal decomposition of the organometallic compound Pt(II)-acetylacetone dissolved in acetone. A high dispersion of platinum to predominantly mono-atomic particles was achieved thanks to the tight fit of the Pt(II)-acetylacetone molecules in the aperture of the zeolite supercage. Using the high angle annular dark field imaging technique of HRTEM, individual Pt particles situated within the zeolite crystals were, for the first time, clearly visible. This offers new possibilities of studying the distribution of incorporated metal particles along the crystal depth.

**Keywords:** HRTEM imaging; impregnation technique; NaX zeolite; Pt(II)-acetylacetone; platinum-modified zeolite.

### INTRODUCTION

Zeolites are aluminosilicates with an ordered open porosity and very developed inner surface area, which approaches several hundred square meters per gram.<sup>1</sup> Aluminum(III) sites present the positive-deficient sites, which are compensated usually by alkali or alkali-earth cations. The charge compensating cations may be replaced by other cationic species by ion-exchange. Zeolites are known as very strong sorbents for molecules interacting with the inner zeolite surface, *i.e.*, those being small enough to penetrate through the cavity orifices.

The cations of transition metals have been introduced into the zeolite cavities either by ion exchange or by impregnation techniques.<sup>2–12</sup> According to numerous literature reports, metals such as Pt, Pd, Ni and Mo, as well as alloys have

\*Corresponding author. E-mail: slavko@ffh.bg.ac.rs

# Serbian Chemical Society member.

doi: 10.2298/JSC0910113M

been incorporated within the cavities of zeolites either by chemical reduction of their cations introduced by ion-exchange or by thermal decomposition of appropriate precursors (in the presence of hydrogen, if necessary).<sup>2</sup> Reducing agents other than hydrogen may be used. For instance, Wang *et al.*<sup>3</sup> introduced Co<sup>2+</sup> ions into the cavities of NaX zeolite and reduced them to metallic Co clusters by means of sodium borohydride.

Considerable catalytic effects of metal-zeolite systems have been demonstrated in numerous, particularly organic, chemical reactions.<sup>13–19</sup> Barthoment,<sup>20</sup> in particular, indicated the role of the aluminosilicate support in suppressing the agglomeration of metal cluster to during prolonged catalyst exploitation.

In various ways, zeolites were the subject of investigations by electrochemical methods.<sup>21–23</sup> Quite recently, zeolites were used as templates to produce metal particle of uniform, sub-nanometer dimensions for electrocatalysis purposes. For instance, Coker *et al.*<sup>11,24</sup> incorporated Pt nanoclusters in NaX zeolite (faujasite type) by the ion-exchange technique, and, upon zeolite dissolution, transferred them to a carbon support to obtain Pt/C electrocatalysts. Furthermore, following literature reports relating to Ag<sup>+</sup>-exchanged zeolites,<sup>10,25</sup> Senthilkumar *et al.*<sup>26</sup> incorporated Pt cluster into the pores of type Y zeolite by cathodic reduction of a previously introduced Pt-salt. They attempted to use so-prepared Pt-loaded zeolite in the form of a membrane for electrochemical reduction of oxygen and oxidation of methanol.<sup>26</sup>

The hitherto published impregnation techniques to incorporate Pt clusters into zeolites involved a solution of Pt(IV) chloride<sup>2,12</sup> or Pt(IV) tetra-aminenitrate<sup>11</sup> as the impregnation agent. Pt(II) acetylacetone was used by Yao *et al.*<sup>27</sup> to synthesize Pt catalysts (0.5–2 % loading) on a mesoporous MCM-41 support. Metal acetylacetones were rarely used in conjunction with zeolites and the studies published to date do not report their decomposition to metals. For example, Ferreira *et al.*<sup>28</sup> investigated NaX zeolite with incorporated Cu acetylacetone, and de Souza *et al.*<sup>29</sup> investigated NaX and NaY zeolites with incorporated Ni acetylacetone, in both cases without their thermal degradation.

The size and shape of metal clusters both in zeolites<sup>4–8</sup> and silicate-based mesoporous materials<sup>9</sup> were examined preferably by high-resolution transmission electron microscopy (HRTEM). The dimensions of metal clusters are expected to be limited by the pore dimensions, for instance, in the case of zeolite, to approx. 1 nm. Many HRTEM microphotographs of zeolites with incorporated metal particles were published,<sup>3–9,11,26</sup> however, they never provided sufficiently clear insight into the distribution of the metal particles along the crystal depth. Usually, insufficient resolution and sample transparency limited the quality of the microphotographs. In some cases, problems arose from the formation of metal clusters of random size on the outer surface of the zeolite crystals,<sup>3,10</sup> as well as

the growth of huge clusters inside the crystals,<sup>7,11</sup> accompanied obviously by destruction of the local zeolite structure.

In this study, NaX zeolite was impregnated with a Pt(II) acetylacetone/acetone solution and the Pt(II) acetylacetone decomposed in order to produce Pt particles within the zeolite cavities. The high angle annular dark field imaging technique of HRTEM, capable of visualizing individual atoms,<sup>30</sup> was used to investigate the distribution of platinum particles within the zeolite crystals.

## EXPERIMENTAL

### *Preparation of platinum-loaded NaX zeolite*

Faujasite type NaX zeolite, with the formula  $\text{Na}_{86}(\text{AlO}_2)_{86}(\text{SiO}_2)_{106}\cdot x\text{H}_2\text{O}$  ( $0 < x < 264$ , depending on the partial pressure of water), approx. 2 g cm<sup>-3</sup> in density, was the product of Linde Co., while Pt(II) acetylacetone ( $\text{Pt}(\text{C}_5\text{H}_7\text{O}_2)_2$ ) was purchased from Aldrich.

A recently published procedure for the thermal decomposition of noble metal acetylacetones to deposit noble metal clusters on the surface of a solid support,<sup>31</sup> which was subsequently adapted to introduce noble metal clusters into zeolite cavities,<sup>32,33</sup> was employed in this study. Briefly, after heating to 350 °C in order to remove adsorbed water and subsequent cooling to room temperature in a dry atmosphere, the zeolite sample was slightly wetted with a dilute acetone solution of platinum(II) acetylacetone. The sample was then dried at 90 °C to evaporate the acetone, and heated at 350 °C under a hydrogen atmosphere to both decompose the Pt(II) acetylacetone and remove its gaseous decomposition products. The impregnation/decomposition procedure was repeated about 20 times until a Pt/zeolite weight ratio of 0.1 was achieved. After this procedure the zeolite was dark brown in color.

### *X-Ray diffractometry*

X-Ray powder diffractograms of the original and Pt-modified NaX zeolite samples were recorded on a Siemens-D500 diffractometer with Ni filtered Cu K $\alpha$  radiation ( $\lambda = 1.54178 \text{ \AA}$ ).

### *Electron microscopy*

Specimens were prepared for transmission electron microscopy by suspending the catalyst powders in ethanol using an ultrasonic bath and adding a drop of the suspensions onto clean holey carbon grids, which were then dried in air. The samples were examined by high angle annular dark field imaging using a Tecnai F20 FEG electron microscope operating at 200 kV. The particle shapes were determined by real space crystallography using high resolution images taken from particles near or on the edge of the carbon black substrate. Conventional bright-field and dark-field imaging were also utilized in order to investigate the overall distribution of the Pt particles. Local structural information from single particles was obtained by numerical Fourier filtering of the digitized image intensity spectrum.

## RESULTS AND DISCUSSION

Usually, the impregnation techniques employed to date for the incorporation of platinum into zeolite cavities involved soaking the zeolite in solutions of inorganic thermodegradable platinum compounds (chloride, tetra-aminonitrate).<sup>2,11,12</sup> The impregnation of NaX zeolite with acetylacetones, although studied experimentally,<sup>32,33</sup> was never considered on the level of molecular structure. This aspect of impregnation will be discussed herein.

As is well known from the literature, the structure of NaX-type zeolite (Fig. 1) consists of small sodalite cages interconnected by means of hexagonal prisms, which together surround almost spherical supercages. The supercages are interconnected mutually by 12-membered rings.<sup>1,34</sup> The inner diameter of the sodalite cages and supercages, with the charge compensating cations placed inside, amount to 0.26 and 0.9 nm, respectively, while their entrance apertures amount to 0.22 and 0.74 nm, respectively.<sup>34,35</sup> Small molecules, such as helium or water, may enter both the sodalite cages and supercages, while even the smallest organic molecules, such as methane, may enter the supercages only. The mean number of molecules which may simultaneously enter a supercage depends on both the volume ratio and molecule geometry. This number is, for example, 5.2 for benzene (planar molecule with a diameter of approx. 0.5 nm) and 3.6 for mezytilene.<sup>36</sup>

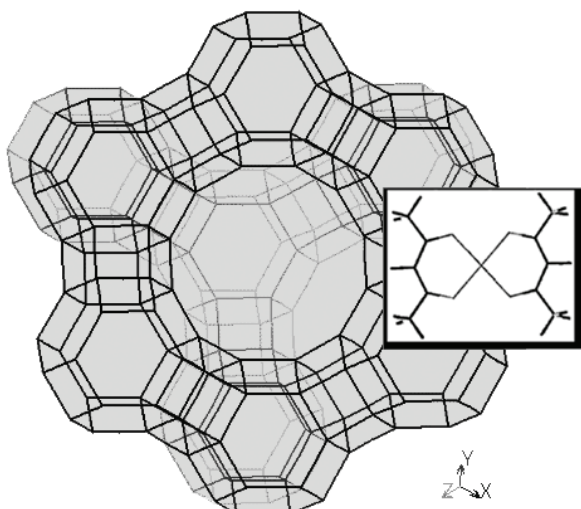


Fig 1. Wire model of the NaX (FAU) zeolite structure, the view directed to the (111) plane, which shows the orifice of a zeolite supercage; a wire model of the planar Pt(II) acetylacetonate molecule in nearly natural proportions is added as an inset.

The structure of the Pt(II)-acetylacetonate molecule is planar.<sup>37</sup> The Pt atom, located at the centre of the molecule, is bonded to the pairs of oxygen atoms of the 2,4-pentanedionato ions *via* one ionic and one coordinative bond, equalized mutually by resonance of the structures. Using Chem3D Ultra (CambridgeSoft) package to analyze intramolecular distances in space, the distance between the centers of the hydrogen atoms situated in the outermost methyl groups along the pentanedione chain, due to their rotation, vary between 0.45 and 0.65 nm. Kenvin *et al.*<sup>37</sup> for Cu(II) acetylacetonate, being similar both in dimensions and in geometry to Pt(II) acetylacetonate, found from monolayer-adsorption measurements on Cab-O-Sil 200 m<sup>2</sup> g<sup>-1</sup> surface that one molecule occupies 0.588 nm<sup>2</sup> of the surface, which is in good agreement with the dimensions 0.65×0.9 nm<sup>2</sup> found

by Chem3D Ultra software for one molecule of Pt(II)-acetylacetone. Therefore, regarding even the van der Waals radii of the hydrogen atoms, the Pt(II) acetylacetone molecule should experience no substantial obstacles when penetrating into the supercages, particularly assuming free rotation of the outermost methyl groups around the C–C bond. This is in accordance with the work of Ferreira *et al.*<sup>28</sup>. Namely, these authors reported that the complex compound Cu(II)-acetylacetone diffuses freely through the channels of NaX zeolite, while complexation of Cu(II) acetylacetone with aliphatic triamines, which led to more voluminous molecules, restricted completely their movement.<sup>28</sup> According to the paper by de Souza *et al.*,<sup>29</sup> the isostructural and dimensionally similar Ni(II) acetylacetone may also be incorporated into NaX zeolite cavities.

This consideration indicates that Pt(II)-acetylacetone may serve effectively as a transporting agent for the incorporation of platinum into NaX zeolite cavities. However, due to its complex configuration and greater dimensions in comparison to benzene,<sup>36</sup> a very low probability for a Pt(II) acetylacetone molecule to enter a previously already occupied supercage. Therefore, the impregnation/thermal decomposition procedure in this case may be considered as the introduction of Pt atoms one after another. The impregnation/thermal decomposition procedure must, therefore, be repeated many times in order to obtain Pt clusters greater than a single atom.

The SEM microphotographs of the zeolite sample used in this study before and after platinum incorporation are shown in Fig. 2. A comparison of these pictures indicates no visible change in the crystal form and mean diameter. However, the platinum-modified sample enabled photographs of better contrast to be taken, indicating better reflectivity to electrons.

Knowledge of the zeolite structure enables the calculation of the population of the supercages by Pt atoms under the assumption of uniform filling. The formula of a unit cell of anhydrous NaX is  $\text{Na}_{86}(\text{AlO}_2)_{86}(\text{SiO}_2)_{106}$  (relative mass 13836). The unit cell is cubic with the length of the axis 2.4975 nm, *i.e.*, roughly 2.5 nm. Thus, one gram of zeolite contains  $3.38 \times 10^{19}$  unit cells. Each unit cell contains 8 supercages, which means  $2.7 \times 10^{20}$  supercages per gram of zeolite.<sup>35</sup> The platinum loaded NaX zeolite sample synthesized in this work contained 0.1 g (*i.e.*,  $3 \times 10^{20}$  atoms) of Pt per gram of NaX. Assuming uniform distribution, Pt-modified NaX zeolite with 10 wt. % of Pt should contain, on average, 1.1 Pt atoms per supercage. Since, according to recent HRTEM observation of Pt nanocrystals, the most reliable diameter of a Pt atom is about 0.26 nm,<sup>38–40</sup> assuming that the sample is transparent, in the present case, particles close to 0.26 nm in size in the plane of the photograph should be seen and, for the case of a quite uniform distribution, on average, 8 individual atoms per unit cell.

The picture shown in Fig. 3 was taken by a high angle annular dark field imaging technique using a Tecnai F20 FEG transmission microscope. This tech-

nique is the best one for observation of atomic arrays of supported nanoparticles of catalyst.<sup>39,40</sup> If the microscope is adjusted to observe platinum, the structural details composed of lighter elements (Si, Al) remain invisible. The microphotograph shown in Fig. 3 is the best picture of a metal-loaded zeolite taken to date, even in comparison to recently published ones.<sup>3,12,24,26</sup>

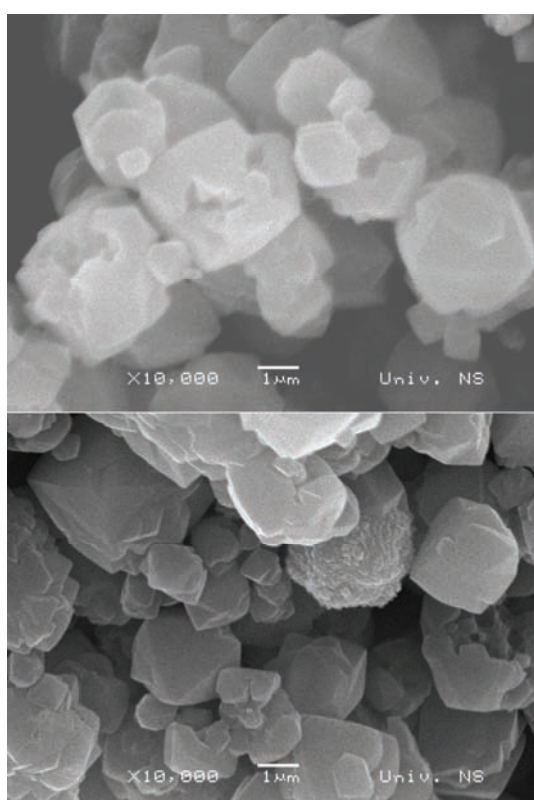


Fig. 2. SEM Microphotographs of the original NaX zeolite (top) and Pt-loaded NaX zeolite (10 wt. % Pt), taken at a magnification of 10000; the mean crystal diameter is approx. 3  $\mu\text{m}$ .

In order to analyze the distribution of particles along unit cells, the transparency of the sample should be discussed.

Aluminum metal of thickness 1.5 and 8  $\mu\text{m}$  is transparent for electrons accelerated to 100 and 1000 keV, respectively. Based on the closeness in the atomic weights, a similar transparency may be expected for silicon. Therefore, for NaX zeolite, being an aluminosilicate material, it may be assumed that, for the 200 keV electron beam used in this study, the depth of transparency is of the order of 1  $\mu\text{m}$ .

Since Fig. 3 presents the tip of a Pt-loaded NaX zeolite monocrystal, from purely geometric considerations, it may be concluded that the largest depth along the axis vertical to the plane of the picture may not exceed 25 nm. Such a depth is

obviously quite transparent for the employed electron beam and, consequently, Fig.3 presents all the Pt particles placed within the piece of zeolite crystal caught by this microphotograph.

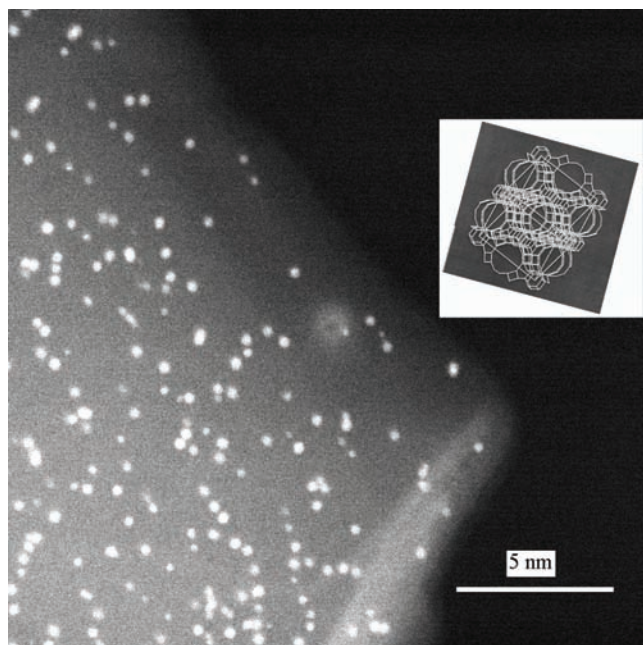


Fig. 3. High angle annular dark field image (200 kV) of a tip of a Pt-loaded NaX zeolite (10 wt. % Pt) monocrystal. Inserted figure presents the model of a (cubic) unit cell of NaX zeolite, with only the Si–Si bonds presented, for sake of clarity. The size and orientation of the model of the unit cell really fits the tip of the photographed crystal.

In the inset of Fig. 3, presents by wire-modeled Si–Si bonds, the details of the structure of a (cubic) NaX unit cell ( $a = 2.5$  nm), in natural proportions to the photographed crystal and properly oriented in space to fit the tip of the photographed crystal. For the photographed crystal, the presented network of Si–Si bonds depicts the real dimensions and positions of the supercages. Based on Fig. 3, statistical analysis of the particle distribution per unit cell may be performed, bearing in mind that the number of unit cells distributed along the electron beam path increases progressively as the distance from the crystal tip increases. Considering the most reliable data for the diameter of a Pt atom,<sup>38–40</sup> Fig. 3 evidences that the number of Pt-atoms per supercage is preferably one, rarely two or three, which might amount to not more than 3 wt. % of the platinum in the zeolite. The missing amount, supplementing the 10 % of platinum in the zeolite, should exist in another form than that perceived in Fig. 3. However, the particles located within

the supercages obviously completely experienced the templating effect of the supercage dimensions.

The dimensions of metal particles incorporated into zeolite crystals were not always limited by the zeolite host.<sup>7,10</sup> For example, silver particles ranging in size from 1 to 18 nm were found in the Faujasite host,<sup>10</sup> which means that silver tends to destroy the local crystal structure and to grow outside the volume of the zeolite cavities. Similarly, Tonscheidt *et al.*<sup>7</sup> observed very large Ir and Rh particles in X zeolite samples modified by ion exchange. They also outlined the problem of instability of the zeolite lattice under the impact of the electron beam during TEM observations.

Additional characterization of the Pt-loaded NaX zeolite sample was realized by means of X-ray diffractometry. The X-ray diffractograms of both the original and platinum-modified NaX zeolite used in this study are shown in Fig. 4. The diffractogram of the original 13 X sample overlaps with the one filed in the JCPDS library.<sup>41</sup> The diffractogram of the Pt-modified sample contains all the diffraction lines visible in that of the original NaX sample. The deviation of the baseline of the X-ray diffractogram over a broad range of  $2\theta$  values is a characteristic feature in this case. A deviation of the baseline of X-ray diffractograms was observed by de Souza *et al.*<sup>29</sup> in the case of NaX zeolite with incorporated Ni(II)-acetylacetone. In terms of crystallography, this feature corresponds to

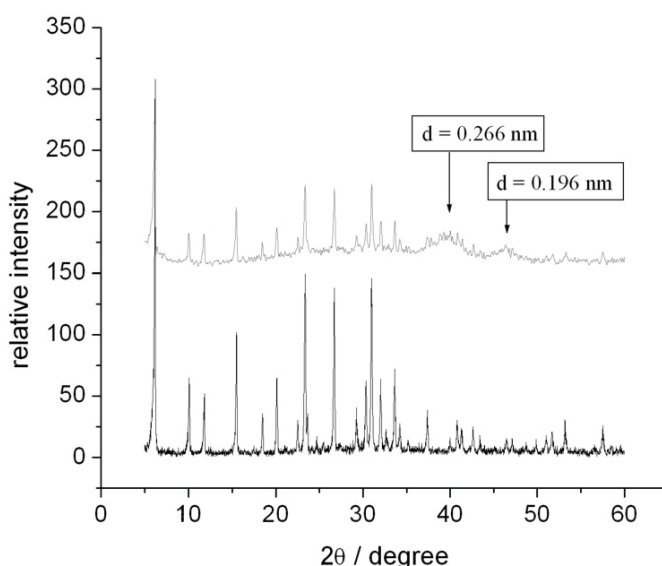


Fig. 4. The X-ray diffractograms of NaX zeolite (lower) and Pt loaded NaX zeolite (upper). The  $d$ -values labeling the humps on the base-line correspond to reflections from the (111) and (200) crystallographic planes of platinum.

amorphization of the sample. It is not due to crushing of the zeolite crystals, since the SEM microphotographs (Fig. 2) taken before and after Pt incorporation did not evidence such an event. Amorphization in this case may be attributed only to slight local deformations of the zeolite lattice caused by the presence of Pt particles. Contrary to data pertaining to NaX zeolite impregnated with Ni-acetylacetone,<sup>29</sup> the amorphization in this case did not influence the adsorption capacity: as proven by thermogravimetry, the adsorption capacity for water was reduced only by the volume occupied by the incorporated platinum.

Based on the microphotograph shown in Fig. 3, which shows that the Pt particles incorporated in the zeolite crystals contain only few atoms, any feature pertaining to the crystal structure of platinum are not to be expected. However, in the diffractogram of the modified zeolite (Fig. 4, upper diagram), two broad humps are visible in the  $35^\circ < 2\theta < 50^\circ$  region, at  $2\theta$  values approaching the angles  $39.75$  and  $46.20^\circ$ . These angles correspond to the two strongest, (111) ( $d = 0.266$  nm) and (200) ( $d = 0.196$  nm), reflections of polycrystalline platinum.<sup>42</sup> The half-width of these humps, with the help of the famous Scherrer formula, show that somewhat larger Pt-particles, with a diameter around 1 nm, also exist in the observed system. Such particles may grow outside of crystal pores by chemical vapor-deposition caused by precursor evaporation during the thermal decomposition procedure. This is in accordance with the fact that a mirror-like layer of platinum condensed on the wall of the glass tube in which the impregnation/decomposition procedure was performed. The simultaneous existence of larger clusters, most probably outside the zeolite crystals, does not distort the finding depicted in Fig. 3 that the procedure employed in this study produces predominantly mono-atomic platinum particles within the zeolite host.

#### CONCLUSIONS

Platinum was incorporated into the cavities of NaX zeolite crystals by multiple impregnations with Pt(II) acetylacetone and its subsequent thermal decomposition. Molecular structure considerations indicate that the Pt(II) acetylacetone molecules may enter the zeolite supercages without molecular rearrangement. However, thanks to the tight fit of the precursor molecule in the supercage orifice, most probably only sequentially may other Pt atoms be introduced inside the zeolite supercages during repetitions of the impregnation/decomposition procedure. This procedure may be characterized as a soft one, which does not cause crushing of the zeolite crystals during the multiple repetitions. The Pt particles were visualized by the high angle annular dark field imaging HRTEM technique, which evidenced that the population of one to a few atoms per supercage prevails.

*Acknowledgement.* The paper was supported by and realized within the projects No. 142047 (S. M.), and No. MHT.2.09.0022.B (Z. M.) of the Ministry of Science of the Republic Serbia.

## ИЗВОД

ЗЕОЛИТ NaX КАО ТЕМПЛАТ ЗА ДОБИЈАЊЕ МОНОАТОМСКИ  
ДИСПЕРГОВАНЕ ПЛАТИНЕ ИМПРЕГНАЦИЈОМ СА РАСТВОРОМ  
Pt(II)-АЦЕТИЛАЦЕТОНАТА У АЦЕТОНУ

СЛАВКО МЕНТУС<sup>1</sup>, ЗОРИЦА МОЈОВИЋ<sup>2</sup> и ВЕЛИМИР РАДИЛОВИЋ<sup>3</sup>

<sup>1</sup>Универзитет у Београду, Факултет за физичку хемију, Студентски торац 12, 11000 Београд, <sup>2</sup>ИХТМ – Центар за катализу и хемијско инжењерство, Његошева 12, 11000 Београд и <sup>3</sup>National Center for Electron Microscopy, Lawrence Berkeley National Laboratory, University of California, Berkeley, USA

Платина је уградњена у кавезе зеолита NaX импрегнацијом и термалним разлагањем органометалног једињења Pt(II)-ацетилацетоната, раствореног у ацетону. Висока дисперзност платине претежно у виду једноатомних честица, постигнута је захваљујући близини димензија молекуле Pt(II)-ацетилацетоната и пречника улазног отвора супекавеза зеолита. Техником широкоугаоне дифракције и тамног поља ултрависокорезолутивне електронске микроскопије, први пут су учињене видљивим индивидуалне честице платине смештене унутар кристала зеолита, што отвара нове могућности у проучавању расподеле уградњених металних честица по дубини кристала.

(Примљено 26. октобра 2008, ревидирано 11. јуна 2009)

## REFERENCES

1. D. W. Breck, *Zeolite Molecular Sieves: Structure, Chemistry and Use*, Wiley, New York, 1974
2. G. H. Kühl, *Modification of Zeolites in Catalysis and Zeolites: Fundamentals and Applications*, J. Weitkamp, L. Puppe, Eds., Springer, Berlin, 1999, p. 81
3. Y. Wang, H. Wu, Q. Zhang, Q. Tang, *Micropor. Mesopor. Mater.* **86** (2005) 38
4. P. Gallezot, I. Mutin, G. Dalmat-Imelik, B. Imelik, *J. Microsc. Spectrosc. Electron.* **1** (1976) 1
5. P. Gallezot, *Surf. Sci.* **106** (1981) 459
6. A. Tonscheidt, P. L. Ryder, N. I. Jaeger, G. Schulz-Ekloff, *Surf. Sci.* **281** (1993) 51
7. A. Tonscheidt, P. L. Ryder, N. I. Jaeger, G. Schulz-Ekloff, *Zeolites* **16** (1996) 271
8. V. Alfredsson, O. Terasaki, Z. Blum, Jan-Olov Bovin, G. Karlsson, *Zeolites* **15** (1995) 111
9. M. Hartman, C. Bischof, Z. Luan, L. Kevan, *Micropor. Mesopor. Mater.* **44–45** (2001) 385
10. J. W. Li, K. Pfanner, G. Calzaferri, *J. Phys. Chem.* **99** (1995) 2119
11. E. N. Coker, W. A. Steen, J. E. Miller, *Micropor. Mesopor. Mater.* **104** (2007) 236
12. B. Imre, I. Hannus, Z. Kónya, J. Kiriczi, *J. Mol. Struct.* **651–653** (2003) 191
13. A. M. Ferrari, K. M. Neyman, T. Bellini, M. Mayer, N. Rösch, *J. Phys. Chem. B* **103** (1999) 216
14. A. L. Yakovlev, K. M. Neyman, G. M. Zhidomirov, N. Rösch, *J. Phys. Chem.* **100** (1996) 3482
15. R. E. Jentoft, M. Tsapatsis, M. E. Davis, B. C. Gates, *J. Catal.* **179** (1998) 565
16. W. A. Weber, B. C. Gates, *J. Catal.* **180** (1998) 207
17. W. A. Weber, B. L. Phillips, B. C. Gates, *Chem. European J.* **5** (1999) 2899
18. W. A. Weber, A. Zhao, B. C. Gates, *J. Catal.* **182** (1999) 13
19. A. G. F. de Souza, A. M. P. Bentes Jr., A. C. C. Rodrigues, L. E. P. Borges, J. L. F. Monteiro, *Catal. Today* **107–108** (2005) 493



20. D. Barthomé, *Catal. Rev.* **38** (1996) 521
21. M. Xu, W. Horsthemke, M. Schell, *Electrochim. Acta* **38** (1993) 919
22. Z. Li, C. M. Wang, L. Persaud, T. E. Mallouk, *J. Phys. Chem.* **92** (1988) 2592
23. C. Iwakura, S. Miyazaki, H. Yoneyama, *J. Electroanal. Chem.* **246** (1988) 63
24. E. N. Coker, W. A. Steen, J. T. Miller, A. J. Kropf, J. E. Miller, *Micropor. Mesopor. Mater.* **101** (2007) 440
25. Y. Zhang, F. Chen, J. Zhuang, Y. Tang, D. Wang, Y. Wang, A. Dong, N. Ren, *Chem. Commun.* (2002) 2814
26. S. Senthilkumar A. Adisa, R. Saraswathi, R. A. W. Dryfe, *Electrochim. Commun.* **10** (2008) 141
27. N. Yao, C. Pinckney, S. Lim, C. Pak, G. L. Haller, *Micropor. Mesopor. Mater.* **44–45** (2001) 377
28. R. Ferreira, M. Silva, C. Freire, B. de Castro, J. L. Figueiredo, *Micropor. Mesopor. Mater.* **38** (2000) 391
29. M. O. de Souza, F. M. T. Mendes, R. F. de Souza, J. H. Z. dos Santos, *Micropor. Mesopor. Mater.* **69** (2004) 217
30. D. O. Klenov, S. Stemmer, *Ultramicroscopy* **106** (2006) 889
31. M. Okumura, T. Tanaka, A. Ueda, M. Haruta, *Solid State Ionics* **95** (1997) 143
32. S. Mentus, Z. Mojović, N. Cvjetičanin, Z. Tešić, *J. New Mater. Electrochem. Syst.* **7** (2004) 213
33. Z. Mojović, S. Mentus, N. Cvjetičanin, Z. Tešić, *Mat. Sci. Forum* **453–454** (2004) 257
34. M. Barrer, A. J. Walzer, *Trans. Faraday Soc.* **60** (1964) 171
35. O. Ursini, E. Lilla, R. Montanari, *J. Hazardous Mater. B* **137** (2006) 1079
36. I. Daems, P. Leflaive, A. Méthivier, G. V. Baron, J. F. M. Denayer, *Micropor. Mesopor. Mater.* **96** (2006) 149
37. J. C. Kenvin, M. G. White, M. B. Mitchell, *Langmuir* **7** (1991) 1198
38. M. Tsuji, P. Jiang, S. Hikino, S. Lim, R. Yano, S.-M. Jang, S.-H. Yoon, N. Ishigami, X. Tang, K. S. N. Kamarudin, *Coll. Surf. A* **317** (2008) 23
39. N. V. Krstajić, Lj. M. Vračar, V. R. Radmilović, S. G. Neophytides, M. Labou, J. M. Jakšić, R. Tunold, P. Falaras, M. M. Jakšić, *Surf. Sci.* **601** (2007) 1949
40. Web Elements, [http://www.webelements.com/periodicity/atomic\\_radius\\_empirical/](http://www.webelements.com/periodicity/atomic_radius_empirical/)
41. Joint Committee on Powder Diffraction Standards (JCPDS), Powder Diffraction File, International Center for Diffraction Data, Swarthmore, PA, 1987, card No. 04-0802.

